Analysis of Steady, Two-Dimensional, Chemically Reacting, Nonequilibrium, Inviscid Flow in Nozzles

R. J. Stiles*
U.S. Air Force Academy, Colorado Springs, Colorado
and
J. D. Hoffman†
Purdue University, West Lafayette, Indiana

A method for solving the equations governing unsteady, two-dimensional, chemically reacting, nonequilibrium, inviscid flow for subsonic, transonic, and supersonic flowfields is described. Steady-state solutions are obtained as the asymptotic solution for large time. Interior points are computed using MacCormack's method, while all boundary points are computed by a reference-plane characteristic method. The finite difference approximation of the species continuity equations is inconsistent in time, but becomes consistent at the steady-state limit. Nonuniform nonequilibrium conditions can specified at the nozzle inlet. Results are presented for a C-H-O-N chemistry system. Computational time is highly problem dependent. For the cases studied to date, converged solutions have been obtained in 5 min to 1 h using a CDC 6500 computer.

Nomenclature

a_f = frozen speed of sound
C_i = mass fraction of species i
C_{pi} = constant pressure specific heat of species i
h = enthalpy
h_i = enthalpy of species i
n = number of chemical species
P = pressure
R_i = gas constant of species i
t = time
T = temperature
u,v = velocity components in the x, y directions
V = velocity magnitude
x,y,t = physical plane coordinate system
$y_c(x)$ = centerbody coordinate
$y_w(x)$ = wall coordinate
ϵ = 0, planar flow; 1, axisymmetric flow
ζ,η,τ = computational plane coordinate system
θ = flow angle
ρ = density
ρ_i = density of species i
σ_i = source function of species i
ψ_k = source term in energy equation

Introduction

PERFORMANCE prediction for a ramjet propulsion system requires a detailed analysis of the flow through each of its major components. This paper presents a procedure[1-3] for calculating the flowfield within the converging-diverging nozzle of a high-speed ($M \approx 6$) ramjet. Under high-speed, high-altitude operating conditions, the ratio of gross nozzle thrust to net engine thrust for a ramjet is quite high (on the order of 5 to 1). Therefore, an important technology requirement for this type of operation is the minimization of nozzle losses. Of the various nozzle loss mechanisms (finite-rate kinetics, vibrational relaxation, nozzle divergence, and boundary-layer effects), finite-rate kinetics effects are particularly important. High temperatures in the combustor and low pressures in the combustor and nozzle affect kinetic losses by significantly increasing the extent of dissociation.

Analysis of the nozzle flowfield can be divided into two parts: analysis of the subsonic/transonic flow in the nozzle entrance and throat regions, and analysis of the supersonic flow in the nozzle divergence. The two parts of the analysis are linked together at a supersonic initial-data line just downstream of the nozzle throat. The effects of finite-rate kinetics must be included in both parts of the analysis. Method of characteristics techniques exist and are recommended for the analysis of the supersonic flowfield.[4,5] Reference 4 can be used for two-dimensional, axisymmetric or planar, steady supersonic flows, and Ref. 5 can be applied to steady supersonic three-dimensional flows. The analysis presented here is for two-dimensional flow in the subsonic and transonic flow regions.

The steady flow solution is obtained as the asymptotic solution to the unsteady equations, with steady flow boundary conditions applied, for large time. The time-dependent technique has been applied successfully to the solution of two-dimensional nonreacting nozzle flow problems by a number of investigators, for example, Migdal et al.[6] and Cline.[7] the basic elements of those references (i.e., governing equations in primitive form, MacCormack's method[8] for interior points, and reference-plane characteristics method at the boundaries) are employed in the present method. The computer code associated with this work is an extension of the VNAP program developed by Cline[7] to include finite-rate chemical kinetics.

The development that follows is applicable to axisymmetric and planar nozzle geometries with or without a centerbody. Nonuniform distributions of equilibrium or nonequilibrium flow properties may be specified at the nozzle inlet. Although the present discussion is focused on ramjet propulsion, the technique is applicable to any subsonic/transonic flowfield where the effects of finite-rate chemical kinetics must be considered.

Modeling the Problem

The distribution of fluid dynamic properties and species concentrations at the nozzle inlet must be provided by the

Presented as Paper 81-1432 at the AIAA/SAE/ASME 17th Joint Propulsion Conference, Colorado Springs, Colo., July 27-29, 1981; received Aug. 6, 1981; revision received April 3, 1984.

*Major, U.S.A.F. Member AIAA.
†Professor of Mechanical Engineering. Member AIAA.

results of a combustor analysis. In the present analysis, it is assumed that the flowfield at the nozzle inlet is a mixture of thermally perfect gases with no condensed phases. The distribution of fluid dynamic properties and species concentrations may be nonuniform across the nozzle inlet, and the flow may be in chemical nonequilibrium. The flow is assumed to be in instantaneous translational, rotational, and vibrational equilibrium. The flow within the nozzle is assumed to be continuous, adiabatic, and inviscid, and body forces are neglected.

Gasdynamic Model

The equations corresponding to the physical model described above are presented by Vincenti and Kruger.[9] These equations are the global continuity, momentum, energy, and species continuity equations, and the thermal and caloric equations of state. In vector form, they are

$$\frac{\partial \rho}{\partial t} + \nabla \cdot (\rho \bar{V}) = 0 \tag{1}$$

$$\rho \frac{\mathrm{D}\bar{V}}{\mathrm{D}t} + \nabla p = 0 \tag{2}$$

$$\frac{\mathrm{D}(h + V^2/2)}{\mathrm{D}t} - \frac{1}{\rho}\frac{\partial P}{\partial t} = 0 \tag{3}$$

$$\frac{\partial \rho_i}{\partial t} + \nabla \cdot (\rho_i \bar{V}) = \sigma_i \qquad (i = 1,\ldots,n) \tag{4}$$

$$P = \rho T \sum_{i=1}^{n} C_i R_i \tag{5}$$

$$h = \sum_{i=1}^{n} C_i h_i \quad \text{where} \quad h_i = \int_{T_0}^{T} C_{pi}\mathrm{d}T + h_i^0 \tag{6}$$

where ρ is the density, $\bar{V}$ the velocity, P the pressure, h the mixture enthalpy including chemical energy, T the temperature, and, for the individual species, ρ_i are the densities, C_i the mass fractions, σ_i the source functions, h_i the enthalpies, R_i the gas constants, C_{pi} the specific heats at constant pressure, and h_i^0 the energies of formation. For steady flow, Eq. (3) requires that the total enthalpy $H_0 = (h + V^2/2)$ remains constant along the streamlines. This fact serves as a useful check on the accuracy of computed results for steady flows.

Equations (3) and (4) can be written in forms which are more convenient for analysis.[1] The energy equation is written in terms of pressure and density rather than enthalpy and kinetic energy, and the species continuity equations are written in terms of species mass fractions rather than species densities. The set of governing equations, written for two-dimensional axisymmetric or planar flow, is

$$\rho_t + u\rho_x + v\rho_y + \rho u_x + \rho v_y + \epsilon \rho v/y = 0 \tag{7}$$

$$u_t + uu_x + vu_y + P_x/\rho = 0 \tag{8}$$

$$v_t + uv_x + vv_y + P_y/\rho = 0 \tag{9}$$

$$P_t + uP_x + vP_y - a_f^2(\rho_t + u\rho_x + v\rho_y) = \psi_k \tag{10}$$

$$C_{it} + uC_{ix} + vC_{iy} = \sigma_i/\rho \qquad (i = 1,\ldots,n) \tag{11}$$

where $\epsilon = 0$ for planar flow and 1 for axisymmetric flow, and

$$\psi_k = \sum_{i=1}^{n} [\gamma_f R_i T - (\gamma_f - 1)h_i]\sigma_i \tag{12}$$

The subscripts in these equations denote partial differentiation. The terms a_f and γ_f are the frozen speed of sound and the ratio of frozen specific heats, respectively. The species continuity equations, Eqs. (11), are coupled to the fluid dynamic equations, Eqs. (7-10), by the energy equation source term ψ_k, which arises as a consequence of finite-rate kinetics.

Since the interior points in this analysis are to be treated by a fixed grid technique, it is necessary to transform the physical space (x,y,t) to a rectangular computational space (ζ,η,τ) in which the differencing is performed, as illustrated in Fig. 1. The following coordinate transformation is employed:

$$\zeta = x, \quad \eta = \frac{y - y_c(x)}{y_w(x) - y_c(x)}, \quad \tau = t \tag{13}$$

where $y_w(x)$ and $y_c(x)$ specify the nozzle wall and centerbody coordinates, respectively. Applying this transformation to Eqs. (7-11) yields the transformed forms of the continuity, momentum, energy, and species continuity equations which are employed in this analysis. Thus,

$$\rho_\tau + u\rho_\zeta + \bar{v}\rho_\eta + \rho u_\zeta + \rho\alpha u_\eta + \rho\beta v_\eta + \epsilon\rho v/\bar{\eta} = 0 \tag{14}$$

$$u_\tau + uu_\zeta + \bar{v}u_\eta + P_\zeta/\rho + \alpha P_\eta/\rho = 0 \tag{15}$$

$$v_\tau + uv_\zeta + \bar{v}v_\eta + \beta P_\eta/\rho = 0 \tag{16}$$

$$P_\tau + uP_\zeta + \bar{v}P_\eta - a_f^2(\rho_\tau + u\rho_\zeta + \bar{v}\rho_\eta) = \psi_k \tag{17}$$

$$C_{i\tau} + uC_{i\zeta} + \bar{v}C_{i\eta} = \sigma_i/\rho \qquad (i = 1,\ldots,n) \tag{18}$$

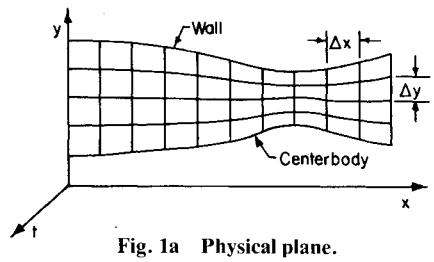

Fig. 1a Physical plane.

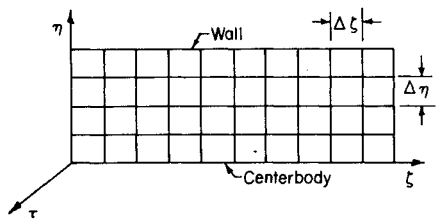

Fig. 1b Computational plane.

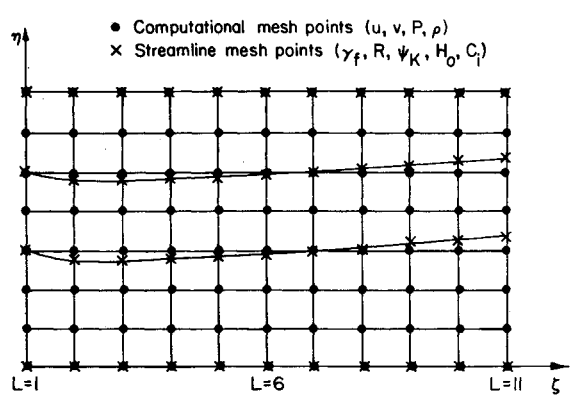

Fig. 2 Computational and streamline mesh points.

where

$$\alpha=\frac{\partial\eta}{\partial x}=-\beta\frac{\partial y_c}{\partial x}-\eta\beta\left(\frac{\partial y_w}{\partial x}-\frac{\partial y_c}{\partial x}\right) \tag{19}$$

$$\beta=\frac{\partial\eta}{\partial y}=\frac{1}{y_w-y_c} \tag{20}$$

$$\bar{v}=\alpha u+\beta v \text{ and } \bar{\eta}=y_c+\eta/\beta \tag{21}$$

Equation (18) may be written as

$$\frac{DC_i}{D\tau}=\frac{\sigma_i}{\rho} \qquad (i=1,\ldots,n) \tag{22}$$

where $DC_i/D\tau$ is the change in C_I following a particle path in the computational plane.

Chemical Kinetics Model

The species source function σ_i appears in the source terms of both the energy equation, Eq. (17), and the species continuity equations, Eqs. (22). Before the species source function can be computed, a reaction mechanism must be specified.

A general reaction equation that may be used to represent any reaction mechanism is

$$\sum_{i=1}^{n}\nu'_{ij}X_i \underset{k_{rj}}{\overset{k_{fj}}{\rightleftharpoons}} \sum_{i=1}^{n}\nu''_{ij}X_i \quad (j=1,\ldots,m) \tag{23}$$

where ν'_{ij} and ν''_{ij} are the stoichiometric coefficients of the reactants and products, respectively, X_i denotes the ith chemical species, and k_{fj} and k_{rj} are the forward and reverse reaction rate coefficients, respectively, for the jth reaction of the m reactions in the reaction mechanism.

Reaction rate coefficients are not readily predicted at the present time; therefore, they are generally determined experimentally. The form for the reverse reaction rate coefficient k_{rj} used in the present analysis is

$$k_{rj}=a_{ij}T^{-n_j}\exp(-b_j/\bar{R}T) \tag{24}$$

where a_{ij}, n_j, and b_j are empirical coefficients, $\bar{R}$ the universal gas constant, and T the local temperature.

Expressions for the species source function σ_i for both dissociation-recombination (D-R) reactions and binary-exchange (B-E) reactions can be developed from the law of mass action.[10] For dissociation-recombination reactions, the species source function $\sigma_{i\text{D-R}}$ is

$$\sigma_{i\text{D-R}}=\bar{m}_i\rho^2\sum_{j=1}^{m}(\nu''_{ij}-\nu'_{ij})\left[K_{j\text{D-R}}\prod_{i=1}^{n}(C_i)^{\nu'_{ij}}-\rho\prod_{i=1}^{n}(C_i)^{\nu''_{ij}}\right]\left(M_jk_{rj}\Big/\prod_{i=1}^{n}(\bar{m}_i)^{\nu''_{ij}}\right) \tag{25}$$

$$K_{j\text{D-R}}=(K_{pj}/\bar{R}T)\prod_{i=1}^{n}(\bar{m}_i)^{\nu''_{ij}}\Big/\prod_{i=1}^{n}(\bar{m}_i)^{\nu'_{ij}} \tag{26}$$

For binary-exchange reactions, the species source function $\sigma_{i\text{B-E}}$ is

$$\sigma_{i\text{B-E}}=\bar{m}_i\rho^2\sum_{j=1}^{m}(\nu''_{ij}-\nu'_{ij})\left[K_{j\text{B-E}}\prod_{i=1}^{n}(C_i)^{\nu'_{ij}}-\prod_{i=1}^{n}(C_i)^{\nu''_{ij}}\right]\left(k_{rj}\Big/\prod_{i=1}^{n}(\bar{m}_i)^{\nu''_{ij}}\right) \tag{27}$$

$$K_{j\text{B-E}}=K_{pj}\prod_{i=1}^{n}(\bar{m}_i)^{\nu''_{ij}}\Big/\prod_{i=1}^{n}(\bar{m}_i)^{\nu'_{ij}} \tag{28}$$

In Eqs. (26) and (28), K_{pj} is the equilibrium constant based on partial pressures, M_j the third-body reaction rate ratio, C_i the species mass fractions, and $\bar{m}_i$ the species molecular weights. The effect of different third bodies on dissociation-recombination reactions is accounted for through the use of third-body reaction rate ratios M_j, as in Eq. (25).

The difficulties in making accurate measurements of the reactions rate coefficients, the necessity of extrapolating experimental data from one situation to another, and the uncertainty as to the reaction mechanism, are all significant factors limiting the accuracy of the analysis presented in this research. However, experience with one-dimensional analyses of reacting flows indicates that the chemical kinetics model used here is adequate for performance prediction.

The reaction mechanism which is used in the present investigation is the same as that used in Ref. 4, but with a provision for the presence of unburned hydrocarbons. This is accomplished by using the following subglobal oxidation step proposed by Edelman and Harsha.[10]

$$C_nH_m+\frac{n}{2}O_2\rightarrow\frac{m}{2}H_2+nCO \tag{29}$$

This reaction proceeds in the forward direction only. The empirical reaction rate coefficient for this reaction is

$$a_j=6.0\times10^4P^{0.3}C^{1/2}_{C_nH_m}C_{O_2} \tag{30}$$

where P has units of atmospheres and C represents species concentrations in g mole/cm^3.

Solution of the Governing Equations

The equations governing the subject problem can be separated into two groups: 1) the equations governing the fluid dynamic variables (i.e., the global continuity, component momentum, and energy equations), and 2) the species continuity equations. For convenience, hereafter the first group will be called the "fluid dynamic equations."

In the present analysis, the steady flow solution is obtained as the asymptotic solution of the unsteady equations with steady flow boundary conditions applied for large time. Introducing finite-rate chemical kinetics into the analysis significantly increases the time required to compute each solution plane, because the number of equations in the mathematical model increases by the number of chemical species considered, and the calculations required to compute the species source function and to integrate the species continuity equations are very time consuming.

The nature of the species continuity equations must be considered in a discussion of computational time. For flows near equilibrium, the species continuity equations are stiff.[11] Standard explicit integration techniques, when applied to stiff differential equations, are unstable except for very small step sizes. The use of implicit methods, however, removes the instability problem and allows more reasonable time steps. In addition to obtaining a solution to the present problem, a significant objective of this research was to achieve the solution in reasonable computational time. To that end, an overall numerical algorithm called the "asymptotically consistent scheme" was developed. That procedure is discussed in the following section.

The Asymptotically Consistent Scheme

Finite difference approximations to differential equations are "consistent" if the finite difference equation yields the differential equation as the step size approaches zero. In the present analysis, the time derivatives of the species mass fractions (i.e., $C_{i\tau}$) are neglected. Consequently, the overall algorithm is inconsistent in the treatment of the species continuity equations, but asymptotically consistent at the steady flow limit where $C_{i\tau}=0$. The procedure is as follows.

The fluid dynamic variables u, v, P, and ρ and the species mass fractions C_i are all known at all computational mesh points (ζ,η) in the initial-data surface at time level N. The fluid dynamic variables are advanced one time step (by the methods of Ref. 7) to time level $N+1$ while the species mass fractions are held constant. Then the flow is assumed to be steady and as many as four streamlines are traced through the flowfield from origins at selected locations across the nozzle inlet. The steady flow forms of the species continuity equations are then integrated along these streamlines from the nozzle inlet to the exit. While more than four streamlines could be used, four yields a reasonable compromise between accuracy and computational time.

The process of advancing the fluid dynamic variables and then integrating the species continuity equations along streamlines is repeated until convergence to the steady flow limit is achieved. This approach is not consistent until the steady state is achieved, because the finite difference forms of the species continuity equations do not approach Eqs. (22) as $\Delta t \to 0$ (i.e., $C_{i\tau}$ is neglected).

Figure 2 illustrates the computational mesh points (ζ,η) and the streamline mesh points. Streamline mesh points are defined by the intersection of streamlines with the constant ζ grid lines. A significant benefit of this approach is that the integration of the species continuity equations always proceeds from computed values of species mass fractions. For example, to integrate from $L=1$ to $L=2$ along a streamline in Fig. 2, one uses known values of fluid dynamic variables and species mass fractions at $L=1$ (computational mesh point) and interpolated values of fluid dynamic variables at $L=2$ (streamline mesh point) to compute the species mass fractions at $L=2$. These computed values are then used in the integration from $L=2$ to $L=3$ along the streamline, etc., to the nozzle exit. The values of ψ_k are computed at all streamline mesh points using the computed values of the species mass fractions. The values of ψ_k at the computational mesh points are calculated by interpolation between the values of ψ_k at the streamline mesh points. Thus, no interpolation for species mass fractions is required anywhere in the entire algorithm.

Contrast this procedure to an unsteady solution scheme where particle paths (for integration of the species continuity equations) are projected rearward from each mesh point at time level $n+1$ to intersect the initial-data surface at time level N. The intersection of this particle path with the initial-data surface will not occur at a computational mesh point, and thus interpolation for fluid dynamic variables and species mass fractions is required in the initial-data plane. The authors of Ref. 4 have noted that interpolation for species mass fractions is likely to produce numerical difficulty in the integration of the species continuity equations. This is not surprising because values of the source terms in the energy and species continuity equations (ψ_k and σ_i, respectively) are very sensitive to variations in the species mass fractions for high temperatures near equilibrium conditions. Therefore, any interpolation error in the values of C_i can produce dramatic errors in these source terms.

The Fluid Dynamic Equations

The procedure for advancing the solution of the fluid dynamic equations (in time) is substantially the same as that employed by Cline.[7] The equations are employed in primitive form, interior points are computed using MacCormack's method,[8] inlet and exit points are computed by a constant-η reference-plane characteristic method, and a constant-ζ reference-plane method is used at wall and centerbody points.

In the constant-η and -ζ reference-plane methods, derivatives with respect to η and ζ are approximated by finite differences and treated as source terms, thus reducing the number of independent variables in the problem by one and yielding a problem in only two independent variables. Characteristic relations are then derived for the resulting equations. Results are summarized in the following discussion of boundary points.

At inlet points, values of H_0, P_0, θ, and C_i are specified, where H_0 is the total enthalpy $(h+V^2/2)$, P_0 the total pressure based on frozen composition at the combustor exit, θ the inlet flow angle, and C_i the species mass fractions. The specification of total conditions at the inlet places an upper limit on the mass and energy of the flow and allows flexibility in the solution for the static properties at the inlet.

Wall and centerbody points are computed using the constant-ζ reference-plane method developed by Cline,[7] modified to include the source term ψ_k in the energy equation.

Exit points are computed for supersonic flow by the constant-η reference-plane method. Cline[7] computed exit points by linear extrapolation from the first and second adjacent interior points. In the present analysis, the computational mesh extends only a short distance into the supersonic flowfield (just far enough so that an accurate supersonic initial-data surface for a steady flow method of characteristics scheme can be computed). The constant-η reference-plane method is used at the exit because it was found to be more accurate than extrapolation in the "barely supersonic" flowfield at the exit.

The Species Continuity Equations

It is well known that integration of the species continuity equations for flows near chemical equilibrium requires special care because the equations become stiff.[11] Cline and Hoffman[5] analyzed and tested a number of integration schemes in their analysis of steady, three-dimensional, chemically reacting, nonequilibrium flow. They concluded that explicit schemes are stable only for very small step sizes. Also, only some of the implicit methods they tested gave adequate results. The method proposed by Lomax and Bailey[12] was chosen as the preferred method. That method was used in the present research. The method is based on a Taylor series expansion of the species continuity equations. It is a second-order accurate implicit method. A complete derivation of the method is given in Ref. 1. The resulting finite difference equation is

$$C_{i\ell+1} = C_{i\ell} + \frac{\Delta s}{2V_\ell}\left[f_{i\ell}\left(3-\frac{V_{\ell+1}}{V_\ell}\right) + \frac{\partial f_{i\ell}}{\partial \rho}(\rho_{\ell+1}-\rho_\ell) + \frac{\partial f_{i\ell}}{\partial T}(T_{\ell+1}-T_\ell) + \sum_{j=1}^{n}\frac{\partial f_{i\ell}}{\partial C_j}(C_{j\ell+1}-C_{j\ell})\right] (i=1,\ldots,n) \tag{31}$$

where Δs is distance along the streamline, $f_i=\sigma_i/\rho$, V the velocity magnitude, and ℓ and $\ell+1$ denote points along the streamline. The partial derivatives in Eqs. (31) are determined analytically. When expanded, Eqs. (31) become a system of n simultaneous, linear, algebraic equations in the n unknowns $K_i = C_{i\ell+1} - C_{i\ell}$, which is easily solved using Gauss elimination. This equation is applied repetitively along streamlines traced through the flowfield. The implicit integration scheme was found by Cline and Hoffman[5] and in the present research to be stable even for large step sizes. However, the method is subject to truncation error, and thus intermediate points are placed between streamline mesh points to reduce the step size used in the integration of the species continuity equations. Since most of the computational time required in the present analysis is devoted to the integration of the species continuity equations, the total integration time is almost directly proportional to the number of intermediate points used.

Relaxation at the Inlet

The total enthalpy H_0, the total pressure based on combustor exit conditions and frozen composition P_0, the flow

angle θ, and the species mass fractions C_i, are specified at each inlet mesh point. The use of total conditions as inlet boundary conditions establishes the energy level of the flow and allows some flexibility in the distribution of the static properties across the inlet. As a result, the distributions of the static properties across the inlet will not necessarily match those across the combustor exit. Discontinuities in static properties between the combustor exit and the nozzle inlet create the need for a relaxation of the species mass fractions between these two points. In an actual flow, there are no discontinuities in the streamwise distributions of the static properties and species mass fractions at the junction between the combustor exit and the nozzle inlet. Therefore, the distributions of σ_i and ψ_k along the flow direction are also continuous at this junction.

The aforementioned discontinuities in the static properties are a consequence of the flow model, i.e., an attempt to link a two-dimensional nozzle analysis to a quasi-one-dimensional combustor analysis. Since the discontinuities do not represent reality, their effect must be minimized at the inlet before the species continuity equations are integrated through the flowfield. This is accomplished by allowing the species mass fractions at the combustor exit to relax to the static conditions at the nozzle inlet for a period of time that minimizes the change in ψ_k between these two points. In effect, a short distance is spliced into the junction between the combustor exit and the nozzle inlet so that the discontinuities in static properties produced by the mathematical model can be replaced with linear gradients. The distance is chosen so that the chemical nature of the flow at the combustor exit (as represented by the energy source term ψ_k) is preserved at the nozzle inlet to the extent possible.

Several important conclusions regarding relaxation of the species mass fractions at the inlet were obtained.

1) For specified gradients in static properties between the combustor exit and the nozzle inlet, ψ_k approaches zero with increasing relaxation time since chemically reacting systems move toward equilibrium with increasing relaxation time.

2) At high temperatures and near-equilibrium conditions, ψ_k is quite sensitive to variations in temperature and density. For example, in the H-F chemistry system, a 10 K temperature perturbation, with no relaxation, can change the computed value of ψ_k by several orders of magnitude.

3) For the chemistry systems and static property gradients studied in this research, relatively small changes in composition occurred during the relaxation from combustor exit to nozzle inlet conditions. Typically, species mass fractions changed by less than 2%.

Failure to relax the species mass fractions at the inlet leads to numerical difficulties for two primary reasons. First, without relaxation, the data set (ρ, T, C_i; $i=1,\ldots,n$) at the inlet is inconsistent. This causes a hard start in the integration of the species continuity equations away from the inlet. Second, if the species continuity equations are not relaxed before the inlet, they will relax within the computed flowfield. This can produce a distribution of ψ_k within the flowfield with large oscillations near the inlet. This ψ_k distribution, in turn, distorts the flowfield, and can even lead to failure of the calculations.

Initial-Data Surface

Several different methods of generating the initial-data surface have been investigated, including:

1) A full one-dimensional finite-rate kinetics solution.

2) One-dimensional, isentropic, constant specific heat ratio solution using representative values of R and γ at the combustor exit followed by integration of the species continuity equations through the resulting one-dimensional flowfield.

3) Same as method 2 above, but with a two-dimensional isentropic solution.

All three methods yielded the same converged solution to the problem in comparable execution times. Since method 2 is the easiest to implement, it is preferred.

Step Size and Stability

No attempt was made to perform a stability analysis for the overall numerical algorithm as applied to the governing equations for unsteady, two-dimensional, chemically reacting, nonequilibrium flow. Stability of the treatment of the equations governing the fluid dynamic variables and stability of the species continuity equation scheme were considered separately. Stability of the overall numerical algorithm was verified by actual computations.

The procedure used to advance the solution for the fluid dynamic equations is subject to the CFL stability criterion.[13] This criterion requires that the finite difference domain of dependence must be at least as large as the continuum domain of dependence. Application of the CFL criterion to unsteady two-dimensional flow yields

$$\Delta\tau \leq 1 \Big/ (V+a)\left(\frac{1}{\Delta\xi^2}+\frac{1}{\Delta\eta^2}\right)^{1/2} \tag{32}$$

The minimum value of the right-hand side of Eq. (32) for the entire flowfield establishes the allowable time step for advancing the fluid dynamic equations.

The second-order implicit scheme used to integrate the species continuity equations was found to be stable for all step sizes. The step size for integration of these equations is not related to $\Delta\tau$ in Eq. (32) since the species continuity equations are integrated along streamlines in space while the fluid dynamic equations are integrated from one time plane to the next.

Overall Numerical Algorithm

The overall numerical algorithm consists of the repetitive and alternate application of the solution techniques previously described for the fluid dynamic equations and the species continuity equations. The solution to the fluid dynamic equations is advanced one time step for a given distribution of the species mass fractions throughout the flowfield. Then the flowfield is assumed to be steady while the species continuity equations are integrated along as many as four streamlines from the nozzle inlet to the exit.

Streamlines are always used along the nozzle wall and centerbody/centerline. The remaining streamlines have their origins at specified computational mesh points (between the wall and centerbody) at the nozzle inlet. Integration of the species continuity equations along streamlines is the most time-consuming portion of the overall algorithm. Therefore, the overall solution should be advanced to near convergence before the third and fourth streamlines are added. Experience with this technique has shown that the addition of streamlines between the wall and centerbody/centerline does refine the solution, but only slightly. For the cases studied to date, there is a rather weak dependence of the fluid dynamic variables on the energy equation source term ψ_k.

For some problems, the fluid dynamic equations may be advanced more than one time step before the species continuity equations are integrated. If this is possible, the total computational time may be reduced significantly.

Convergence is achieved when the computed values of the fluid dynamic variables and the species mass fractions no longer change with time (within a specified tolerance).

Verification

At the present time there are no other methods available for the analysis of two-dimensional, chemically reacting, nonequilibrium, subsonic and transonic inviscid nozzle flows. Therefore, it was not possible to make comparisons with existing results. However, a number of verification tests were performed.

The scheme for integrating the species continuity equations must generate accurate concentration profiles for specified distributions of the fluid dynamic variables along the streamlines. To test this capability, one-dimensional analyses

of several kinetics problems were performed using the ODK (One-Dimensional Kinetics) program.[14] Using the distributions of ρ, T, and V from those results, the species continuity equations were integrated through the given flowfields by the present algorithm. The resulting concentration profiles compared very favorably with those computed by ODK. Differences in species concentrations between ODK and the present algorithm were most significant at the nozzle throat. However, for two different chemistry systems (C-H-O-N and H-F) in several nozzle geometries, the differences in individual species concentrations never exceeded 3.4%.

There are four conditions that must be satisfied by a converged solution and which are therefore useful for determining the accuracy of the computed results. First, the law of conservation of mass requires that the mass flow at each axial position along the nozzle must be constant. Values of mass flow at the nozzle inlet, throat, and exit were computed and made available for comparison.

Second, at the steady-state limit, the total enthalpy H_0 must be constant along streamlines in the flowfield. To assess this requirement, a total enthalpy error was used as a measure of the accuracy of the solution. It is defined as

$$H_0 \text{ error} = \frac{H_{0L} - H_{0R}}{(V_E^2 - V_I^2)/2} \tag{33}$$

where H_{0L} is the total enthalpy at axial position L along a given streamline, H_{0R} the total enthalpy at the combustor exit for the same streamline, and V_E and V_I the velocity magnitudes at the nozzle exit and inlet, respectively, along the streamline. Thus, "H_0 error" indicates the local deviation from the enthalpy level at the nozzle inlet (along a given streamline) normalized with respect to the change in kinetic energy along the streamline. Profiles of total enthalpy error for the cases studied are presented with the discussion of results.

Third, the sum of the species mass fractions must be unity throughout the flowfield. This fact is not used explicitly in the problem formulation or in the numerical algorithm. However, the sum of the species mass fractions at each axial mesh point along the kinetics streamlines was computed as a check.

Fourth, the finite-rate kinetics results must lie between the equilibrium and frozen solutions, since those cases correspond to infinite and zero reaction rates, respectively.

For further verification of the present analysis, results of the present technique were mass averaged (in the radial direction) and compared with ODK results. Mass-averaged temperature profiles are compared with one-dimensional temperature profiles in the Results section.

For the final verification of the present analysis, the present algorithm was employed to calculate the steady two-dimensional supersonic flowfield in a 15-deg conical nozzle. The results were compared with those from the steady two-dimensional method of characteristics solution obtained by the TDK (Two-Dimensional Kinetics) program.[4] The results of an H-F system subsonic-transonic analysis were used to

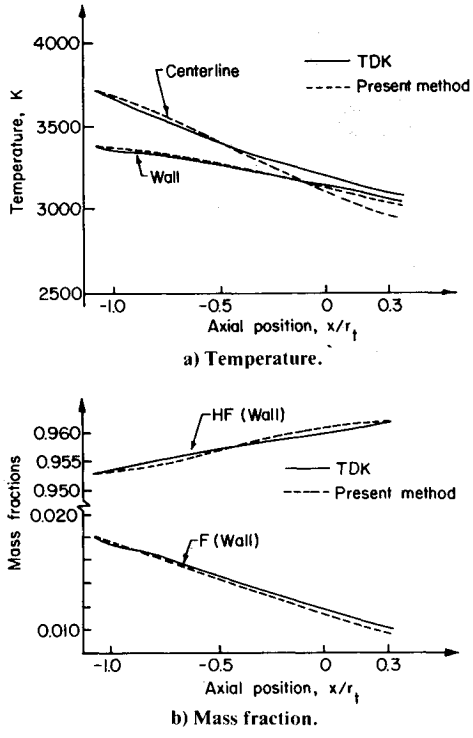

a) Temperature.

b) Mass fraction.

Fig. 3 Verification with the TDK computer program.

Table 1 C-H-O-N reaction mechanism

$H_2O + H \rightleftharpoons H_2 + OH$	$H_2O + M \rightleftharpoons OH + H + M$
$H_2O + O \rightleftharpoons 2OH$	$H_2 + M \rightleftharpoons 2H + M$
$OH + H \rightleftharpoons H_2 + O$	$O_2 + M \rightleftharpoons 2O + M$
$OH + O \rightleftharpoons O_2H$	$CO_2 + H \rightleftharpoons OH + CO$

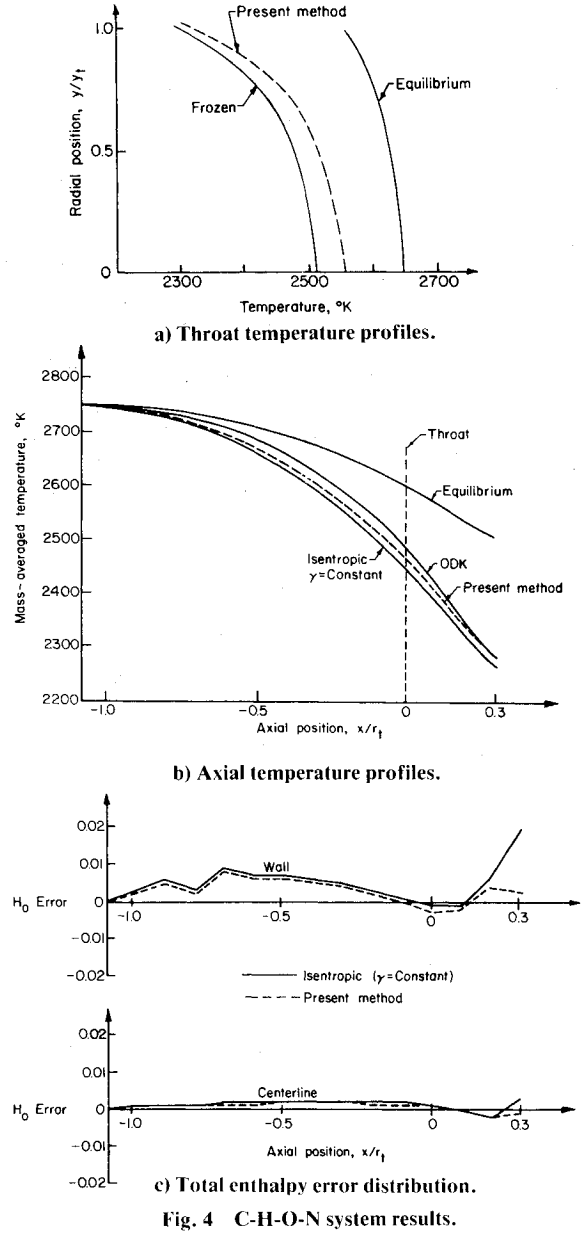

a) Throat temperature profiles.

b) Axial temperature profiles.

c) Total enthalpy error distribution.

Fig. 4 C-H-O-N system results.

generate the initial-data line for both the method of characteristics solution and the solution by the present algorithm. The reaction mechanism recommended in Ref. 4 was employed. Eight equally spaced mesh points were used along the initial-data line. A representative comparison of the results is presented in Fig. 3 (TDK denotes the characteristics solution). Note the excellent agreement in the temperature and concentration profiles along the wall and the fair agreement of the centerline temperature profile.

Results

Several different nozzle geometries and chemistry systems were analyzed using the present method. Results are presented here for only one chemistry system (i.e., C-H-O-N) and one nozzle geometry. References 1-3 present results for two other chemistry systems (i.e., C-H-O-N with unburned propane and H-F).

The C-H-O-N system was analyzed because of its applicability to ramjet propulsion. The reaction mechanism considered is presented in Table 1. The nozzle considered is a circular-arc throat conical nozzle with a 19.05-cm inlet radius, a 12.065-cm throat radius, a 12.065-cm throat radius of curvature, a 45-deg convergence angle, and a 15-deg divergence angle. The nozzle exit is 3.535 cm downstream of the throat. The gas composition at the nozzle inlet corresponds to the equilibrium composition of the products of combustion of a typical hydrocarbon fuel in air. Although nitrogen is present in the gas mixture, it is assumed to be chemically inert. Thus, it participates in the energy transfer process, but not the reaction mechanism. Some selected results from that study are presented in Fig. 4.

Figure 4a presents throat radial temperature profiles compared with frozen and equilibrium results. The two-dimensional character of the flowfield is evident. Figure 4b presents axial mass-averaged temperature profiles compared with frozen, equilibrium, and ODK results. The mass-averaged temperature profile for the finite-rate kinetics solution does fall between the equilibrium and frozen solutions and matches the ODK solution[14] quite well. In this case, there is only a small departure from the frozen solution. For both the present and frozen solutions, a mass flow difference between the inlet and the throat values of 0.8% occurred in the converged results. For the present method, the sum of the species mass fractions deviated by less than 0.000001 along both the wall and centerline streamlines.

The profiles of total enthalpy error for the kinetics solution are compared to those for an isentropic ($\gamma = \text{const}$) solution in Fig. 4c. The error is less than 1% at all mesh points except for the isentropic solution at the last wall point. This particular point is just downstream from the junction between the circular arc in the throat region and the conical section in the nozzle divergence. Experience indicates that the discontinuity in the second derivative of the wall coordinates at this junction causes distortion in the total enthalpy profile. Adding three more mesh points in the axial direction and recomputing the isentropic solution reduces the total enthalpy error at the original location to 1%. The addition of finite-rate chemical kinetics to this problem has not significantly affected the profile of "H_0 error" with respect to the isentropic ($\gamma = \text{const}$) results.

With 18 mesh points along the ζ axis, two chemical kinetics streamlines, and five intermediate points specified along streamlines, each integration of the species continuity equations for the C-H-O-N system required approximately 11 s on the CDC 6500 computer. For the same conditions, each additional streamline adds about 4 s to the integration time.

Integration of the species continuity equations after each time step, with two streamlines and five intermediate points, yielded an acceptable solution in a computational time of approximately 1 h. However, for this system, it is possible to integrate the species continuity equations as infrequently as once every 30 time planes. This reduces the computational time to approximately 5 min.

Conclusions

A technique for the analysis of two-dimensional subsonic and transonic inviscid nozzle flow including the effects of finite-rate chemical kinetics, starting from nonuniform nonequilibrium conditions at the nozzle inlet, has been developed. It provides an accurate flowfield solution into the supersonic flow region which can be used to generate an initial-data line (or surface) for multidimensional method of characteristics analyses. The procedure, when coupled with a method of characteristics scheme for supersonic nozzle flows, should provide a highly accurate analysis of the entire nozzle flowfield.

Computational time is highly problem dependent. It is especially sensitive to the number of chemical species and reactions in the chemistry model, the use of the intermediate points (between streamline mesh points) in the integration of the species continuity equations, the number of chemical kinetics streamlines used, and the frequency with which the species continuity equations are integrated through the flowfield as the solution is advanced forward in time. For the cases which have been analyzed to date, solutions have been obtained in 5 min to 1 h using a CDC 6500 computer.

Acknowledgment

This work was sponsored by the AFWAL Aero Propulsion Laboratory under Contract F33615-79-C-2065. The Project Engineer was John R. Smith (AFWAL/PORT).

References

[1] Stiles, R. J., "Analysis of Steady, Two-Dimensional Chemically Reacting Nonequilibrium Flow by an Unsteady, Asymptotically Consistent Technique," Ph.D. Thesis, School of Mechanical Engineering, Purdue University, W. Lafayette, Ind., May 1980.

[2] Stiles, R. J. and Hoffman, J. D., "Analysis of Steady, Two-Dimensional, Chemically Reacting Nonequilibrium Flow by an Unsteady, Asymptotically Consistent Technique. Vol. I, Theoretical Development. Vol. II, Computer Program Manual," AFWAL-TR-81-2127, Sept. 1982.

[3] Stiles, R. J. and Hoffman, J. D., "Analysis of Steady, Two-Dimensional, Chemically Reacting Nonequilibrium Flow by an Unsteady Asymptotically Consistent Technique," AIAA Paper 81-1432, July 1981.

[4] Kliegel, J. R., Nickerson, G. R., Frey, H. M., Quan, V., and Melde, J. E., "ICRPG Two-Dimensional Kinetic Reference Program," Dynamic Science, Monrovia, Calif., July 1968.

[5] Cline, M. C. and Hoffman, J. D., "The Analysis of Nonequilibrium, Chemically Reacting, Supersonic Flow in Three Dimensions," AFAPL-TR-71-73, Aug. 1971.

[6] Migdal, D., Klein, L., and Moretti, G., "Time-Dependent Calculations for Transonic Nozzle Flow," *AIAA Journal*, Vol. 7, Feb. 1969, pp. 372-374.

[7] Cline, M. C., "VNAP: A Computer Program for the Computation of Two-Dimensional, Time-Dependent Compressible, Viscous, Internal Flow," Los Alamos Scientific Laboratory, Los Alamos, N. Mex., Rept. LA-7326, Nov. 1978.

[8] MacCormack, R. W., "The Effect of Viscosity in Hypervelocity Impact Cratering," AIAA Paper 69-354, April 1969.

[9] Vincenti, W. G. and Kruger, C. H. Jr., *Introduction to Physical Gas Dynamics*, John Wiley & Sons, New York, 1965, Chaps. VII and VIII.

[10] Edelman, R. B. and Harsha, P. T., "Laminar and Turbulent Gas Dynamics in Combustors—Current Status," *Progress in Energy Combustion Science*, Vol. 4, 1978, pp. 1-62.

[11] Curtiss, C. F. and Hirshfelder, J. O., "Integration of Stiff Equations," *Proceedings of the National Academy of Science*, Vol. 38, 1952, pp. 235-243.

[12] Lomax, H. and Bailey, H. E., "A Critical Analysis of Various Numerical Integration Methods for Computing the Flows of a Gas in Chemical Nonequilibrium," NASA TN D-4109, Aug. 1967.

[13] Courant, R., Friedrichs, K. O., and Lewy, H., "Uber die Partiellen Differenzialgleichungen der Mathematischen Physik," *Mathematische Annalen*, Vol. 100, 1928, pp. 32-74.

[14] Frey, H. M., Kliegel, J. R., Nickerson, G. R., and Tyson, J. T., "ICRPG One-Dimensional Kinetic Reference Program," Dynamic Science, Monrovia, Calif., July 1968.